THE JOURNAL OF BIOLOGICAL CHEMISTRY
Vol. 276, No. 45, Issue of November 9, pp. 41648–41655, 2001

Printed in U.S.A.

Mutational Analysis of the Different Bulge Regions of Hepatitis C Virus Domain II and Their Influence on Internal Ribosome Entry Site Translational Ability*

Received for publication, May 8, 2001, and in revised form, July 13, 2001
Published, JBC Papers in Press, August 9, 2001, DOI 10.1074/jbc.M104128200

Federico Odreman-Macchioli, Francisco E. Baralle‡, and Emanuele Buratti

From the International Centre for Genetic Engineering and Biotechnology, 34012 Trieste, Italy

The hepatitis C virus (HCV) 5′-untranslated region and, in particular, domains II to IV are involved in the internal ribosome entry site (IRES) structure. Recent structural evidence has shown that the function of domain II may be to hold the coding RNA in position until the translational machinery is correctly assembled on the decoding site. However, a comprehensive mutational and functional study concerning the importance of the different RNA regions that compose domain II is not yet available. Therefore, we have taken advantage of the recently proposed secondary structure of domain II to design a series of specific mutants. The bulge regions present in the latest secondary structure prediction of domain II were selectively deleted, and the effects of these mutations on IRES translation efficiency were analyzed. Our results show that the introduction of these mutations can variably affect the degree of HCV translation, causing a moderate to total loss of translation ability that correlates with the severity of changes induced in the RNA secondary structure and degree of p25 ribosomal protein UV cross-linking, but not with the ability of the 40S ribosomal subunit to bind the IRES. These findings support the proposed structural role of domain II in HCV translation.

Translation initiation in hepatitis C virus (HCV)[1] is strongly dependent on a highly conserved RNA structure located at the 5′-end of its genome known as the internal ribosome entry site (IRES). The presence of this IRES allows the 40S ribosomal subunit to position itself directly on the starting AUG codon, allowing a cap-independent mechanism of translation initiation (1, 2). The functional studies performed to this date on both cellular and viral IRES elements have shown that there is a necessity to maintain specific sequence and structural elements in the proper conformation and position to allow correct assembly of the translational machinery, as recently reviewed in Refs. 3 and 4. In fact, the HCV IRES is able to fold in a complex secondary structure closely resembling that of the recently isolated GB virus B (5, 6), with four domains (I to IV) (7, 8), a helical structure (9), and a pseudoknot (10) (see Fig. 1 for a schematic diagram). The recent crystallographic and structural analyses have revealed that these elements fold upon themselves to adopt a unique tertiary structure that can bind the 40S-eukaryotic initiation factor 3 complex with high affinity (11–16). For this reason, past analyses have highlighted the importance of maintaining the structural integrity of domains II, III, and IV (7–10, 17–24) and the unstructured domains (25) to retain efficient protein translation, as recently reviewed in Ref. 26.

The majority of mutational studies performed in the past have been focused on domain III, the largest secondary structure of the HCV IRES (17, 19–21, 23, 27), and domain IV, which includes part of the HCV core protein coding sequence and the initiator AUG codon in a stem-loop configuration (7, 28–30). Several cellular factors such as eukaryotic initiation factor 3 (14, 20, 31, 32), La autoantigen (33–35), heterogeneous ribonucleoprotein L (36), poly-C binding protein (37, 38), and poly-pyrimidine-binding protein (39–41) have been recently reported to bind in these regions and influence translation initiation. It should be noted that although functional preinitiation complexes can be assembled on the HCV IRES even in the absence of any of these factors (14, 31), variations in cellular levels of these proteins may be the reason for the recent observations that IRES activity *in vivo* is dependent on the cell cycle (42) and cell type (43).

In contrast to domain III, considerably less is known concerning the importance of the different regions of domain II, principally due to the fact that several alternative RNA secondary structures have been proposed in recent years (7, 8, 44). These changes have made it difficult to compare past mutational studies (22) with the latest structural model, which is based not only on structural analyses but also on the phylogenetic comparison with recently isolated HCV-related viruses (hog cholera virus, GB virus B, and bovine viral diarrhea virus) (8). Therefore, we have introduced a comprehensive series of mutations and deletions in the single-stranded regions of this domain II structure (see Fig. 1). The mutants were then analyzed for their ability to direct IRES translation, the degree of p25 ribosomal protein UV cross-linking, their ability to bind the 40S ribosomal subunits (in sucrose gradient assay and footprinting analysis), and changes in secondary structure.

EXPERIMENTAL PROCEDURES

Plasmid Construction of the Different 5′-UTR Mutants—All mutants described in this study were constructed by polymerase chain reaction, and the primer sequences are shown in Table I. All mutants were amplified from a template plasmid containing nucleotides 1–920 described in detail elsewhere (20). All mutants were prepared in pBluescript II KS+ (Amersham Pharmacia Biotech) using the primers in the following combination: 1) for mutants Δ53-55 and Δ108-110, domIIaS/reverse and domIIaAS/universal primer; 2) for mutants Δ61-64 and Δ103, domIIbS/reverse primer and domIIbAS/universal primer; and 3) for mutants Δ71-73 and Δ93-96, domIIcS/reverse and domIIcAS/universal primer. Both amplification products were mixed in the same molar

* The costs of publication of this article were defrayed in part by the payment of page charges. This article must therefore be hereby marked "*advertisement*" in accordance with 18 U.S.C. Section 1734 solely to indicate this fact.

‡ To whom correspondence should be addressed: International Centre for Genetic Engineering and Biotechnology, Padriciano 99, 34012 Trieste, Italy. Tel.: 39-40-3757337; Fax: 39-40-3757361; E-mail: baralle@icgeb.trieste.it.

[1] The abbreviations used are: HCV, hepatitis C virus; IRES, internal ribosome entry site; DTT, dithiothreitol; MAb, monoclonal antibody; UTR, untranslated region; wt, wild type.

proportion and subjected to a second round of amplification using the universal and reverse primers. To obtain the double mutants, the same group of primers was used on single deletion mutants rather than the original template. To prepare the different set of AUG mutants, we used the primers described in Table I using the same strategy described above, using the 5′-wt and the Δ71-73 mutant as template. All constructs were fully sequenced before their *in vitro* transcription using Beckman CEQ 2000 Dye Terminator Cycle Sequencing according to the manufacturer's instructions.

UV Cross-linking and Secondary Structure Determination—All Bls KS+ plasmids described in this study were linearized by digestion with *Hin*dIII. Transcription of 2 μg of linearized plasmid was performed in the presence of [α-^{32}P]UTP (Amersham Pharmacia Biotech). The specific activities of these labeled RNA preparations were in the range of 4×10^6 cpm/μg RNA. The UV cross-linking technique, preparation of the ribosomal salt wash extract from COS-1 cells, and secondary structure analysis using RNase V1, RNase T1, and S1 nuclease have already been described in detail in a previous work (21). Briefly, the UV cross-linking assay was performed by adding [α-^{32}P]UTP-labeled RNA probes (2×10^5 cpm/incubation) in a water bath for 15 min at 30 °C with 18 μg of the ribosomal salt wash extract (or 6 pmol of purified 40S subunits) in a 20-μl final volume. Final binding conditions were 20 mM Hepes, pH 7.9, 72 mM KCl, 1.5 mM $MgCl_2$, 0.78 mM magnesium acetate, 0.52 mM DTT, 3.8% glycerol, 0.75 mM ATP, and 1 mM GTP. In the competition experiments, cold RNA was also added as a competitor 5 min before the addition of the labeled RNAs (the amount used is reported in the figure legends). Samples were then transferred into the wells of an HLA plate (Nunc; InterMed) and irradiated with UV light on ice (0.8 J, approximately 5 min) using a UV linker (Euroclone). Unbound RNA was then digested with 30 μg of RNase A (Sigma) and 6 units of RNase T1 (Sigma) by incubation at 37 °C for 30 min in a water bath. Samples were then analyzed by 12% SDS-polyacrylamide gel electrophoresis followed by autoradiography, drying, and exposure to Kodak X-Omat AR films for 12–24 h. Films were then scanned on a Macintosh G3 work station using Adobe Photoshop and printed using a Phaser 400 printer.

Transfection Analysis of the Different Mutants in COS-1 Cells—The different mutants were then excised from the Bls KS+ plasmids by cutting with *Xba*I-*Hin*dIII restriction enzymes and inserted in the pSV growth hormone bicistronic expression system for transfection experiments in COS-1 cells as described previously (20). Briefly, COS-1 cells at 60% confluence were transfected with 2 μg of each plasmid using *N*-[1-(2,3-dioleoyloxyl)propyl]-*N,N,N*-trimethylammoniummethyl sulfate (Roche Molecular Biochemicals). After 48 h, the cells were collected, and the hGH levels were quantified by an enzyme-linked immunosorbent assay kit (Roche Molecular Biochemicals) and used to normalize the amount of cellular lysate in the Western blot procedures. The amount of reporter core protein produced was recognized using MAb B12.F8 and detected on Kodak autoradiographic film by enhanced chemiluminescence analysis (ECL; Amersham Life Science) according to the manufacturer's instructions. The film was subsequently scanned using an Imaging Densitometre GS-670 (Bio-Rad), and each band was quantified using the molecular Analyst program for the Macintosh computer. Each transfection was repeated three times. When the two core protein isoforms (the 23-kDa processed and the 25-kDa unprocessed forms) were present, they were quantified together.

Sucrose Density Gradients of Binary IRES-40S Complexes and Enzymatic Footprinting Analysis—The purification of 40S ribosomal subunits and the assembly of binary IRES-40S ribosomal complexes were performed essentially as described previously by Odreman-Macchioli *et al.* (21). Briefly, 40S ribosomal subunits were prepared from HeLa extracts by precipitation for 4 h at 4 °C and centrifugation at 30,000 rpm in a Beckman 60Ti rotor and resuspended in buffer A (20 mM Tris-HCl, pH 7.6, 2 mM DTT, and 6 mM $MgCl_2$) with 0.25 M sucrose and 150 mM KCl to a concentration of 40 A_{260} units/ml. This suspension was incubated with 1 mM puromycin (Sigma) for 10 min at 0 °C and then incubated for 10 min at 37 °C before the addition of KCl to 0.5 M final concentration. The 40S and 60S ribosomal subunits were then separated by centrifugation of 2-ml aliquots of this suspension through a 10–30% sucrose gradient in buffer A with 0.5 M KCl for 17 h at 4 °C and 22,000 rpm, using a Beckman SW28 rotor. The 40S subunits were precipitated from the pooled gradient fractions by centrifugation for 18 h at 4 °C and 50,000 rpm in a 60Ti rotor. Pellets were resuspended in buffer B (20 mM Tris-HCl, pH 7.6, 0.2 mM EDTA, 10 mM KCl, 1 mM DTT, 1 mM $MgCl_2$, and 0.25 M sucrose) to a final concentration of 60 A_{260} units/ml. Ribosomal complexes were assembled by incubating 2×10^5

TABLE I
Primers used for polymerase chain reaction amplification

Primer	Sequence (5′→3′)
domIIaS	CCCTGTGAGGTACTGTCTTC
domIIaAS	GTCCTGGAGGCACGACACTC
domIIbS	GGATCTACTGCACGCAGAAA
domIIbAS	AGGCTGCACGCACTCATACT
domIIcS	TCTTCACGCAAGCGTCTAGC
domIIcAS	ACGACACTCATACTAACGCC
domII76S	GCAGAAAGCCGCTAGCCATG
domII76AS	CATGGCTAGCGGCTTTCTGC
domII82S	AGCGTCTAAAAATGGCGTTA
domII82AS	TAACGCCATTTTTAGACGCT
domIII260S	AGTAGTGTTGCGTCGCGAAA
domIII260AS	TTTCGCGTCGCAACACTACT
domIII290S	ACTGCCTGATGGGGTGCTTG
domIII290AS	CAAGCACCCCATCAGGCAGT
AUG339S	ACCGATGACCAAAAGCACGA
AUG339AS	TCGTGCTTTTGGTCATCGGT
AUG345S	ACCGTGCACCAAAAGCatgA
AUG345AS	TCATGCTTTTGGTGCACGGT

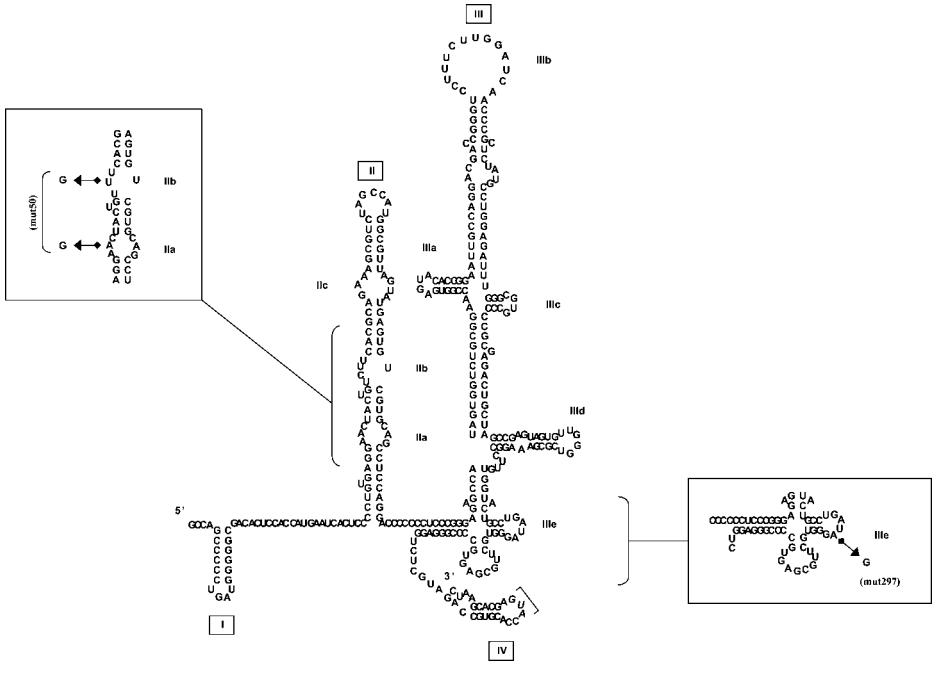

FIG. 1. **Schematic representation of HCV IRES.** Schematic representation of the HCV 5′-UTR secondary structure including part of the initiation coding sequence. The *boxed regions* contain the two initial mutations analyzed: mut50 (A54G and U63G) and mut297 (A297G). The principal domains are indicated by roman numerals *I* to *IV*, and single subdomains are also indicated. The translation initiator AUG is indicated by the *bracket*.

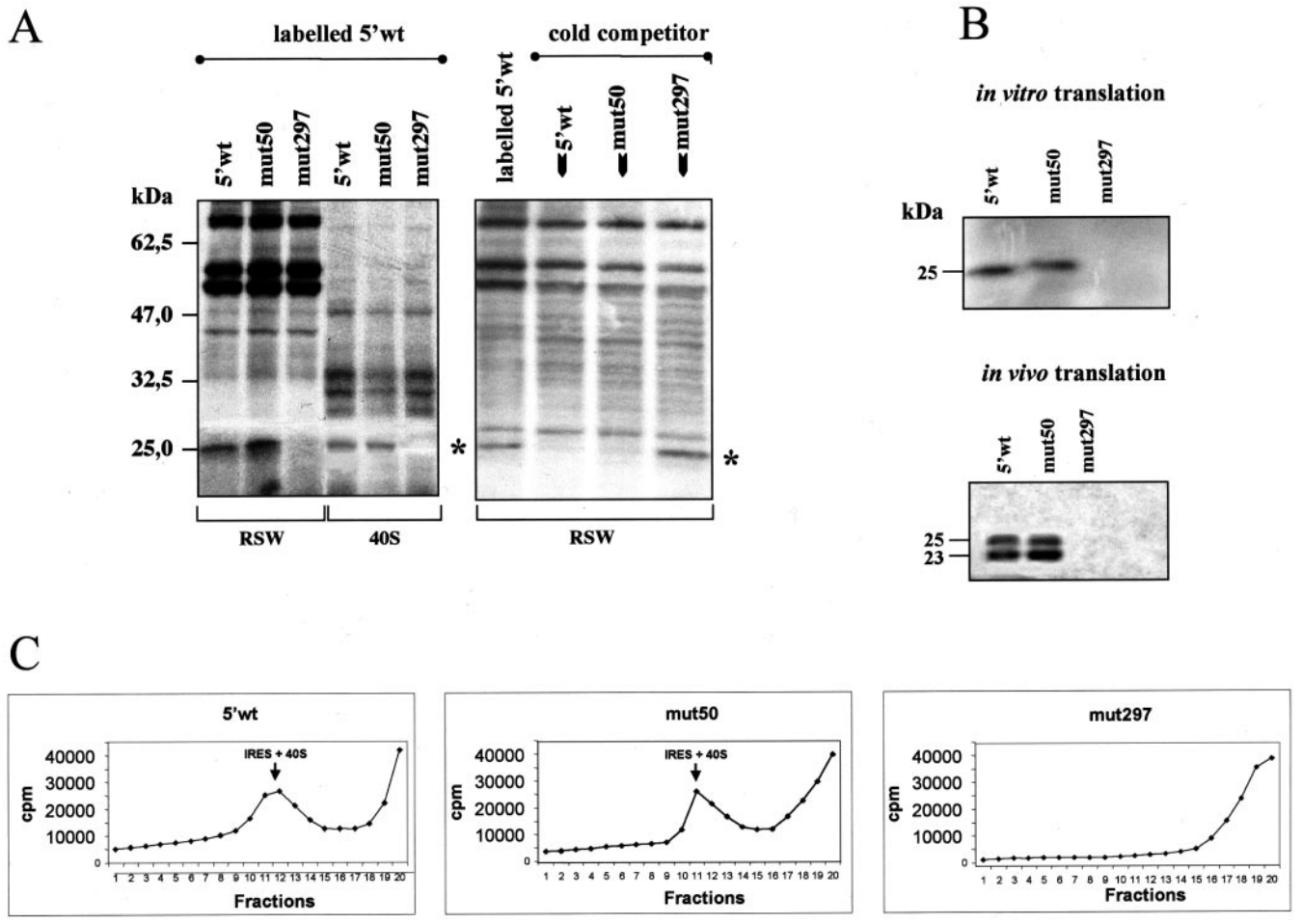

FIG. 2. **Analysis of domain II initial single-point mutations.** *A* (*left panel*) shows a UV cross-linking assay using COS-1 ribosomal salt wash extract (*RSW, lanes 1–3*) and a purified HeLa 40S ribosomal subunit extract (*40S, lanes 4–6*) in the presence of labeled mut50, mut297, and 5′-wt RNAs. A 25-kDa protein is observed to bind only to mut50 (*lanes 2* and *5*) and 5′-wt (*lanes 1* and *4*) but not to mut297 (*lanes 3* and *6*). The *right panel* shows a competition experiment using cold 5′-wt, mut50, and mut297 RNA in the presence of labeled 5′-wt and ribosomal salt wash (*lane 1,* no competitor). Each cold RNA was used at 5× molar excess. The position of the 25-kDa ribosomal protein is indicated by an *asterisk*. *B* shows the *in vitro* and *in vivo* IRES activity of each mutant assayed both in a rabbit reticulocyte lysate system (*top panel*) and in a transfection assay in COS-1 cells (*bottom panel*). In the first assay, only the unprocessed ^{35}S-labeled HCV core protein is visualized by autoradiography, whereas in the second assay, the processed (23-kDa) and nonprocessed (25-kDa) HCV core proteins are visualized by Western blot. The two proteins were recognized using MAb B12.F8 and detected with enhanced chemiluminescence staining. *C* shows an analysis of the binary IRES-40S ribosomal complex formation on 5′-wt, mut50, and mut297 labeled RNAs. Assays were performed on a 10–30% sucrose density gradient with purified 40S ribosomal subunits. The position of the binary complexes is indicated by an *arrow*. Sedimentation was from *right* to *left*.

cpm of labeled RNAs for 10 min at 30 °C in a 100-μl reaction volume that contained buffer E (2 mM DTT, 100 mM potassium acetate, and 20 mM Tris, pH 7.6) with 2.5 mM magnesium acetate, 100 units of RNasin (Promega), 1 mM ATP, and 6 pmol of 40S subunits. The complexes were resolved by centrifugation through a 10–30% sucrose gradient in buffer E with 6 mM magnesium acetate for 16 h at 4 °C and 24,000 rpm, using a Beckman SW41 rotor. The radioactivity of gradient fractions was determined by Cerenkov counting. The enzymatic footprinting analysis was performed basically as described previously by Kolupaeva *et al.* (15). The IRES-40S ribosomal complexes were assembled in 20-μl reaction volumes by mixing 6 pmol of 40S subunits with 2×10^5 cpm of labeled RNAs in binding buffer (20 mM Tris-Cl, pH 7.5, 2.5 mM magnesium acetate, 100 mM KCl, and 2 mM DTT). Free or 40S-IRES RNA complexes were digested by incubation for 10 min at 30 °C with RNase T1 (Sigma) at a final concentration of 0.02 unit/μl (in the absence or presence of the 40S ribosomal subunit). The end-labeled primer 5′-TTCGTGCTCATGGTGCACGGT-3′ (complementary to HCV nucleotides 332–352) was annealed to RNA, and the extended cDNA products (using Moloney murine leukemia virus reverse transcriptase according to standard protocols) were analyzed by electrophoresis on 8% polyacrylamide-7 M urea gels and exposed to X-Omat film (Kodak) after they were dry.

RESULTS

The recent mutation/deletion studies performed on the lower portions of HCV 5′-UTR domain III have highlighted the existence of a very close relationship between RNA structure and IRES translational ability. Indeed, even single-nucleotide changes in selected regions (IIId and IIIe) have been reported to completely abolish IRES activity (17, 27). It was therefore interesting to determine whether an analogous situation could also be found in any of the single-stranded regions of HCV domain II. Therefore, two substitutions (A54G and U63G) were inserted in the IIa and IIb bulges of domain II (mut50), as shown in Fig. 1. As control, we used a second mutant (mut297) carrying an A297G substitution in stem-loop IIIe, a mutation that was previously described to abolish IRES activity (27). Each mutant was then analyzed for translational ability (both *in vitro* and in transfection assay), for complexing with the 40S ribosomal subunit, and for binding to a p25 ribosomal protein. This p25 protein has been previously identified as a ribosomal protein by several independent studies (21, 31, 45) (15). In particular, Pestova *et al.* (31) had identified this 25-kDa protein as ribosomal protein S9 through internal sequence analysis. However, in a recent article (46) this identification has been queried, and it has been suggested by immunoprecipitation analysis that the ribosomal p25 protein corresponds to another ribosomal protein of similar molecular mass, ribosomal protein

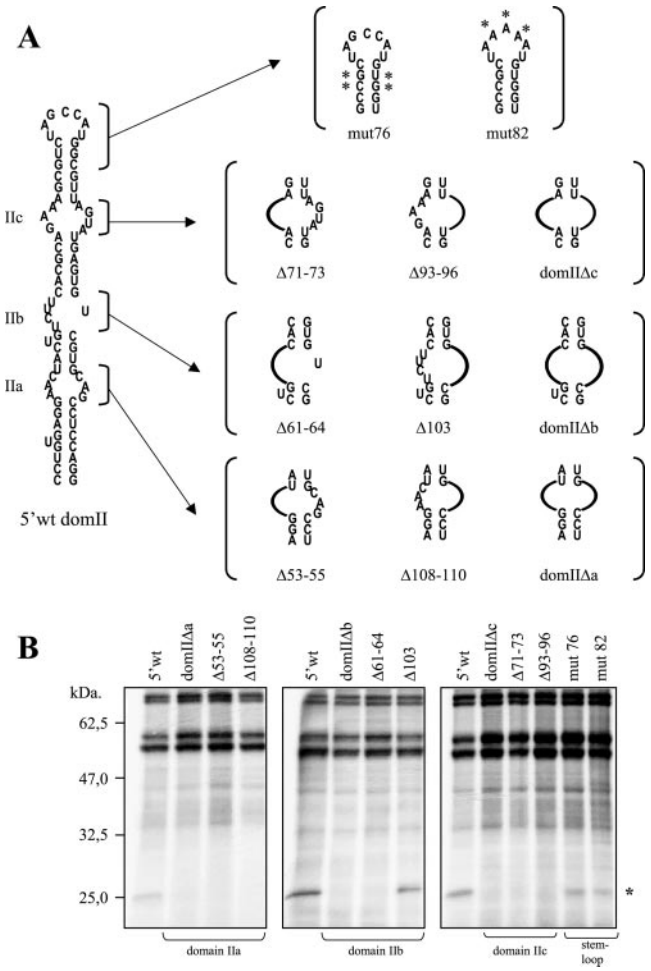

FIG. 3. **Schematic representation of domain II deletion mutants and ribosomal protein p25 cross-linking.** *A* shows a schematic representation of the wild type domain II of HCV 5′-UTR and of the mutant structures used in this study. The *arrows* indicate how each series of mutants was obtained from the original 5′-wt sequence by selectively deleting the three bulge regions either partially or completely. In addition, two mutants in the apical stem-loop region of domain II (mut76 and mut82) are shown. *B* shows a UV cross-linking analysis of all reported mutants in the presence of COS-1 ribosomal salt wash extract. The *asterisk* indicates the position of the p25 ribosomal protein.

S5. The binding of this protein is of interest because p25 is the only protein described thus far whose degree of UV cross-linking changes following mutations in the domain II region (22). Fig. 2*A* (*left panel, lanes 1–3*) shows a UV cross-linking assay using a ribosomal salt wash protein extract (*RSW*) with each labeled RNA. The results show that UV cross-linking of a p25 protein can be observed for the wild type (5′-wt) and mut50, but not for mut297. The same result is obtained using a purified 40S subunit preparation (*40S*) as shown in Fig. 2*A* (*left panel, lanes 4–6*).

A competition analysis was also performed to confirm the specificity of this interaction. Fig. 2*A, right panel,* shows that in keeping with the direct binding assays only cold 5′-wt and mut50 RNAs (but not cold mut297 RNA) can compete for the binding of this protein to the HCV IRES. Both mutants were then analyzed for their ability to drive IRES translation. In the case of mut297, we observed a total inhibition in the translation of the HCV core protein both *in vivo* and *in vitro,* whereas mut50 showed a level of translation comparable with the wild type (Fig. 2*B, top* and *bottom panels*). It should be noted that the HCV core protein isoforms that are produced in transfection are slightly larger than normal (25/23 kDa as opposed to 23/21 kDa) due to the addition of a C-terminal tag sequence, as described previously (47). We then analyzed by sucrose density gradient the ability of the 40S ribosomal subunit to bind to these mutant RNAs. Fig. 2*C* shows that mut50 binds the 40S ribosomal subunits with the same efficiency of the wild type RNA (5′-wt). On the other hand, mut297 was totally incapable of binding the 40S ribosomal subunits, a result that is totally consistent with the recent crystallographic data that identify IIId, IIIe, and IIIf as the regions that contact the 40S platform (13).

Because these single-nucleotide mutations in domain II did not affect the translational ability of the HCV IRES, we then prepared a new set of mutants in which all domain II bulge regions (IIa, IIb, and IIc) were partially or completely deleted. In addition, we prepared two additional mutants in the upper region of domain II to test the importance of this upper stem-loop portion. A schematic representation all these mutants is reported in Fig. 3*A*. We then tested the degree of UV cross-linking of the p25 ribosomal protein. Fig. 3*B* shows that all deletions introduced in the IIa, Iib, and IIc bulges abolished the UV cross-linking signal from the p25 ribosomal protein, with the exception of a single-nucleotide deletion in bulge IIb (Δ103) and in the two upper stem-loop mutants (mut76 and mut82). To investigate the effect of these mutations on the efficiency of the HCV-IRES translation, we transfected each mutant in COS-1 cells in the pSV GH bicistronic system (20), which used the HCV core protein itself as reporter protein. Fig. 4*A* shows that the translation efficiency of these mutated IRESs was variable. In particular, mutants domIIΔa, Δ53-55, and Δ93-96 showed an almost complete lack of IRES translation. On the other hand, mutants Δ108-110, domIIΔb, Δ61-64, domIIΔc, and Δ71-73 retained an intermediate level of IRES activity (ranging between 21% and 33%) (Fig. 4*B*). Finally, the mutants that showed no decrease or little decrease in the degree of p25 cross-linking (mut76 and mut82 and mutant Δ103) showed translation efficiencies comparable to that of the 5′-wt (Fig. 4*B*). The reactivity of MAb B12.F8 with the enhanced chemiluminescence substrate and HCV core protein was determined by preparing a standard calibration curve using a recombinant flock house virus protein displaying the B12.F8 epitope (FHV-C3) on its surface, as described previously (48). The results, which are shown in Fig. 4*C,* were used to quantify the amount of core protein produced in each transfection experiment.

We then tested whether this variability in IRES activity was the result of an incorrect assembly of the 40S-IRES binary complex. However, sucrose density centrifugation analysis performed by mixing labeled RNA with purified 40S subunit showed that all mutants were capable of complexing with the ribosomal subunit (Fig. 5). The similarity of all 40S-5′-UTR binary complex profiles in the sucrose gradient analysis suggested that none of the mutations introduced in domain II could affect the binding of the 40S subunit to the HCV RNA, a result that is consistent with a recent study in which no changes in binding affinity of the 40S subunit were measured for an IRES in which the entire domain II has been deleted (14). However, to rule out the existence of subtler changes in the 40S subunit positioning on the HCV IRES, we performed footprinting analysis on two representative mutants (Δ71-73 and domIIΔa) that displayed 30% IRES activity and no IRES activity, respectively. The analysis, shown in Fig. 6*A,* demonstrates that the inhibition of RNase T1 cleavages on the IIId region (*GGU 265–267*) after incubation with the 40S ribosomal subunit is identical in all three IRESs, irrespective of their translational ability.

Furthermore, the work of Rijnbrand *et al.* (28) had shown that when scanning is involved in the recognition of the trans-

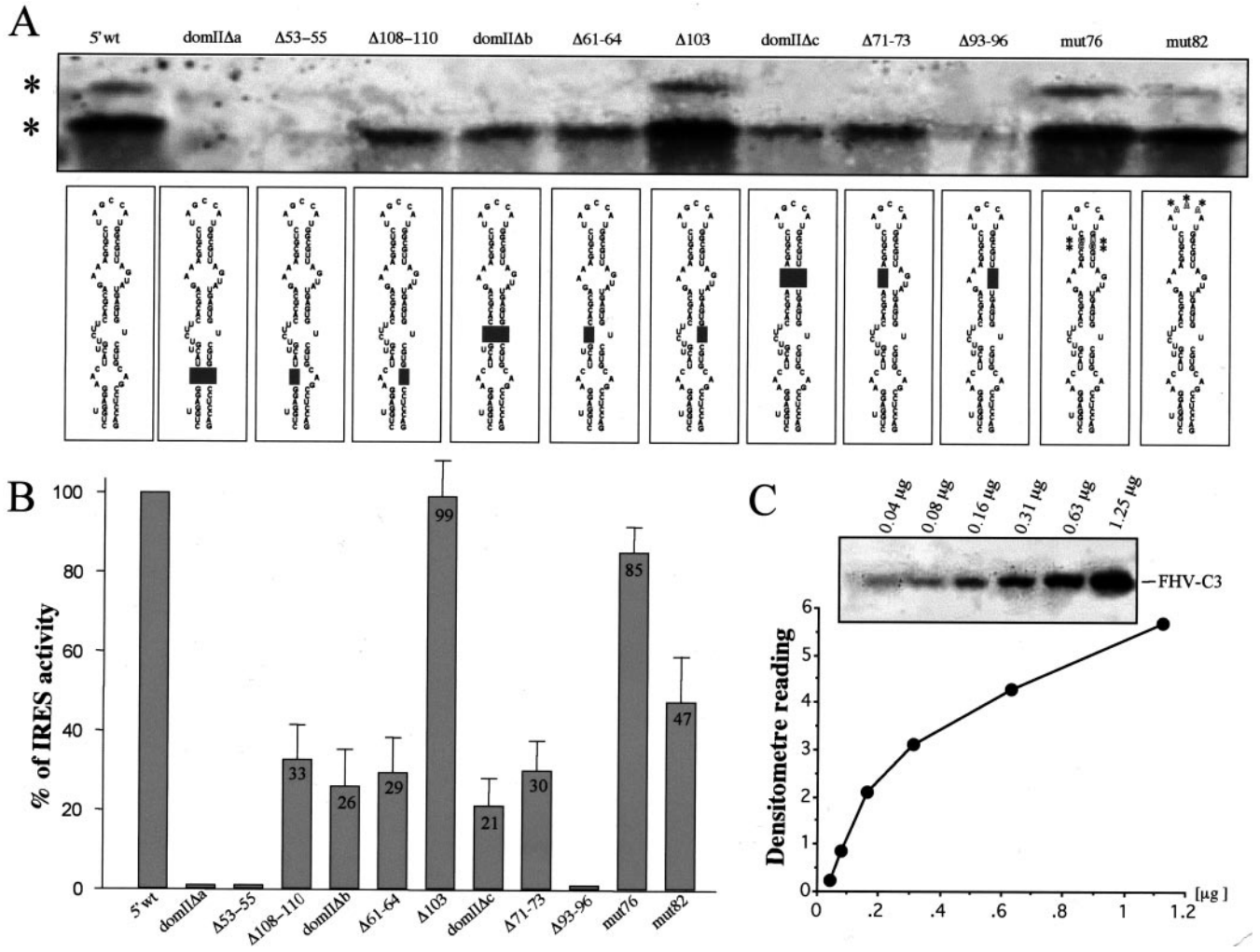

FIG. 4. **Translational ability of domain II mutants in transient transfection analysis.** *A* (*top panel*) shows a Western blot following a transfection assay in COS-1 cells of the different 5′-UTR mutants used in this study. The two bands (indicated by an *asterisk*) represent the processed (23-kDa) and unprocessed (25-kDa) core proteins, which were recognized using MAb B12.F8 and visualized by enhanced chemiluminescence staining. In the *bottom panel* of *A,* a schematic representation of these different domain II mutants is reported for easier reference. *B* shows a quantification of the amount of core protein produced by each mutant (with respect to the wild type sequence) obtained in three independent transfection experiments (including S.E.s). The average value obtained from each mutant is included *inside* each respective *bar*. *C* shows a standard calibration curve to calculate MAb B12.F8 reactivity with different amounts of HCV core protein. The standard calibration curve was obtained by blotting increasing quantities of a flock house virus protein (FHV-C3) displaying the B12.F8 epitope on its surface (*inset*).

lation initiating AUG (at position 341), it is limited to a narrow region between nucleotides 335 and 350. Therefore, a possible shift in ribosome positioning following mutations in the domain II region could consequently cause a more efficient selection of AUG in alternative positions with respect to the wild type. For this purpose, the AUG in the wild type IRES and the Δ71-73 mutant was shifted by 3 nucleotides in either the downstream or upstream direction, and the original AUG was inactivated by a AUG to AAA mutation. The Δ71-73 mutant was chosen on the basis that it displayed an intermediate level of IRES efficiency (30%) that made it ideal to detect eventual further losses (or improvements) after the shift in AUG positioning. However, as shown in Fig. 6*B,* transfection analysis of these mutant IRESs demonstrated that in all cases, the ability to translate is completely abolished.

Finally, to find further differences that might correlate with the translational efficiency of these mutants, the influence of these two deletions (Δ71-73 and domIIΔa) on the domain II secondary structure was measured. A secondary structure analysis of these two mutants was then performed using double-stranded (RNase V1) and single-stranded specific (RNase T1 and S1 nuclease) enzymes, as reported in Fig. 7. First of all, it should be noted that the control cleavages in the wild type domain II are completely consistent with the latest structural model (8). Most interestingly, deletion of the Δ71-73 region results in a substantially small degree of structural change. In particular, the only difference from the wild type structure is represented by the appearance of a prominent T1 cleavage in correspondence to the G present in the other half of the IIc bulge (nucleotides 93–96). Nonetheless, cleavage of the apical bulge (nucleotides 80–86) in the Δ71-73 is unchanged as compared with the wild type, and the V1 cleavages are consistent with a conservation of the double-stranded wild type regions. On the other hand, after deletion of the IIa bulge (domIIΔa), the secondary structure of domain II undergoes a drastic structural change that eliminates most of the RNase cleavages that were obtained for the wild type domain.

DISCUSSION

Initiation of translation of hepatitis C virus RNA is a cap-independent process, which involves an IRES element that mediates internal entry of the ribosome (26). There are several IRES strategies used by different viruses, and in this respect, the HCV IRES has recently been shown to employ a unique

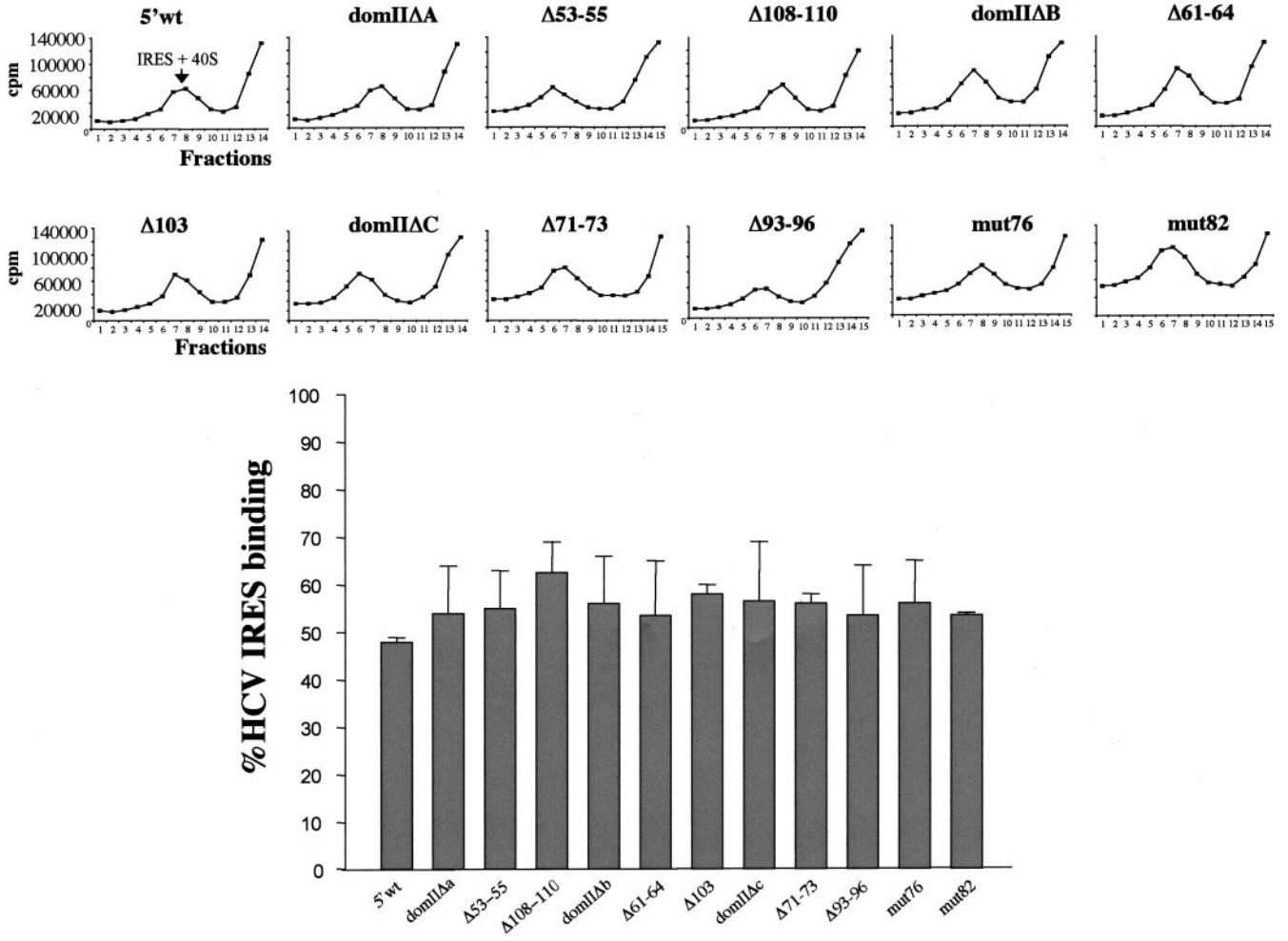

FIG. 5. **Sucrose gradient analysis of 40S-IRES ribosomal complexes of domain II mutants.** Sucrose gradient centrifugation analysis of each domain II mutant. The *arrows* indicate the binary IRES-40S ribosomal complexes. Assays were performed on a 10–30% sucrose gradient with labeled RNAs and purified 40S ribosomal subunit. Complexes were resolved by centrifugation through a 10–30% sucrose gradient. The radioactivity of gradient fractions was determined by Cerenkov counting. Sedimentation was from *right* to *left*. The results from three independent experiments were analyzed, and the average amount of labeled IRES RNA migrating with the 40S ribosomal fraction was calculated for each mutant. The results, including S.E.s, are shown in the *bottom graph*.

method of ribosome recruitment (14, 31). The recently published structural map of the HCV IRES bound to the 40S ribosome obtained using cryoelectron microscopy (13) has substantially increased our insight into the role played in the translation mechanism by each of the IRES domains. In particular, domain II was found to be responsible for the induction of a conformational change in the 40S subunit that could play an important role in translation initiation by holding the HCV coding RNA in the decoding site of the ribosome in position until the translational machinery is correctly assembled (13).

It should be noted that mutational analysis has been used in the past to determine whether specific domain II nucleotide sequences were important for efficient IRES translation (22). However, the design of these experiments was based on an older domain II structure, and the results of these experiments are now difficult to interpret because the position of the stem and bulges has changed considerably from those initial predictions (7, 8, 44). In this study, we report the results of a systematic mutational study concerning the importance of the RNA regions present in the latest secondary structure proposed for domain II.

Sucrose gradient analysis of the IRES-40S complexes formed by the mutants under study showed that all variant sequences had comparable ability to form valid complexes. This result was confirmed by footprinting analysis on selected mutants. This conclusion is consistent with a recent study that analyzed an HCV IRES mutant in which domain II had been entirely deleted, and this deletion did not result in any change of 40S binding affinity to the HCV IRES (14). Nonetheless, almost all our deletions have the ability to decrease the degree of UV cross-linking of a p25 ribosomal protein to the HCV RNA, a possible indication that in these mutants, the 40S conformational change has not taken place (13). This decrease in IRES efficiency is particularly evident with the modifications in the IIa region. Interestingly, in the model by Spahn *et al.* (13), this region is mapped near the location of the coding RNA in the mRNA binding groove. It is therefore tempting to speculate that our result reflects this close association. However, correlation between loss of p25 degree of UV cross-linking and translational ability is not complete. In fact, in several mutants in which p25 UV cross-linking was abolished, we have observed a small to moderate translation efficiency. Secondary structure analysis of these mutants has shown that a correlation can be established between maintenance of correct domain II secondary structure and translational ability.

The importance of secondary structure is also evident from the fact that single-point mutations in the different bulges (mut50 and Δ103) and small changes in the single-stranded region of the apical stem-loop (mut82) do not seem to affect translation ability. In this respect, it should be noted that the

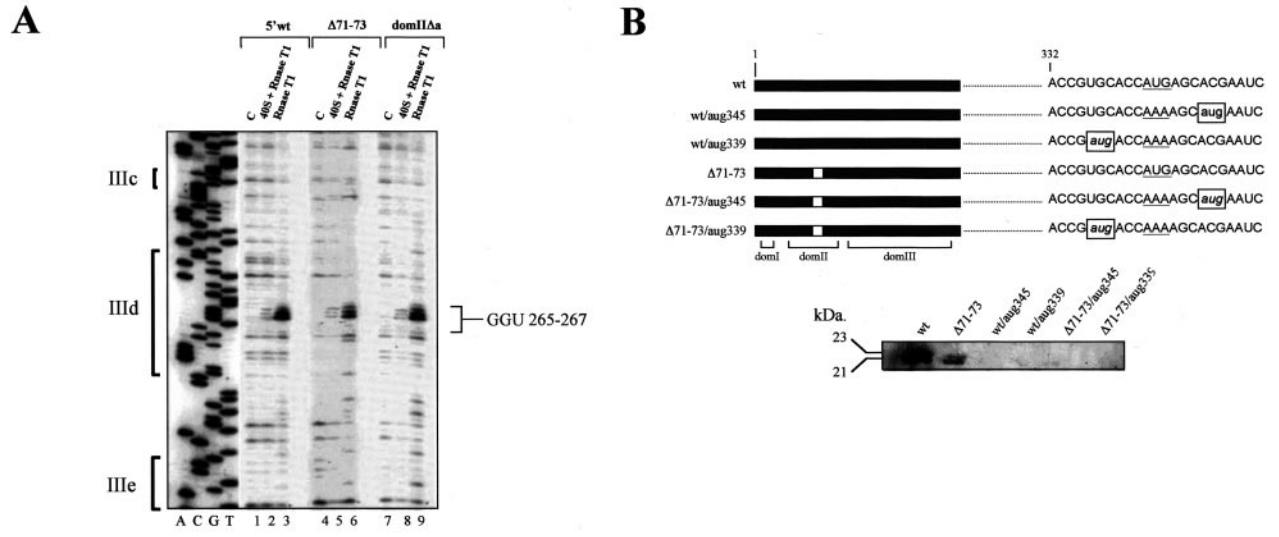

FIG. 6. **Footprinting analysis of wild type and mutant 40S-IRES complexes and effects of AUG shift on translation activity.** *A* shows an enzymatic footprinting of the 40S-IRES complex of the 5′-wt, Δ71-73, and domΔIIa. The cDNA products obtained by primer extension were run on a polyacrylamide gel to show the RNase T1 sensitivity of these RNAs either alone (*lanes 2, 5,* and *8*) or in the presence of the 40S subunit (*lanes 3, 6,* and *8*). A dideoxy sequence using the same primer of the reverse transcription extension analysis was run in parallel. The protected region (*GGU 265–267*) is indicated on the *right*. *B* shows the translation efficiency of four AUG mutants (wt-aug339, wt-aug345, Δ71-73/aug339, and Δ71-73/aug345) in which the initiator AUG was mutated to AAA, and a novel AUG codon (*boxed* in the schematic diagrams) was introduced three nucleotides away either in the 5′ or the 3′ direction. The amount of reporter core protein synthesized by each mutant was determined by Western blot using MAb B12.F8.

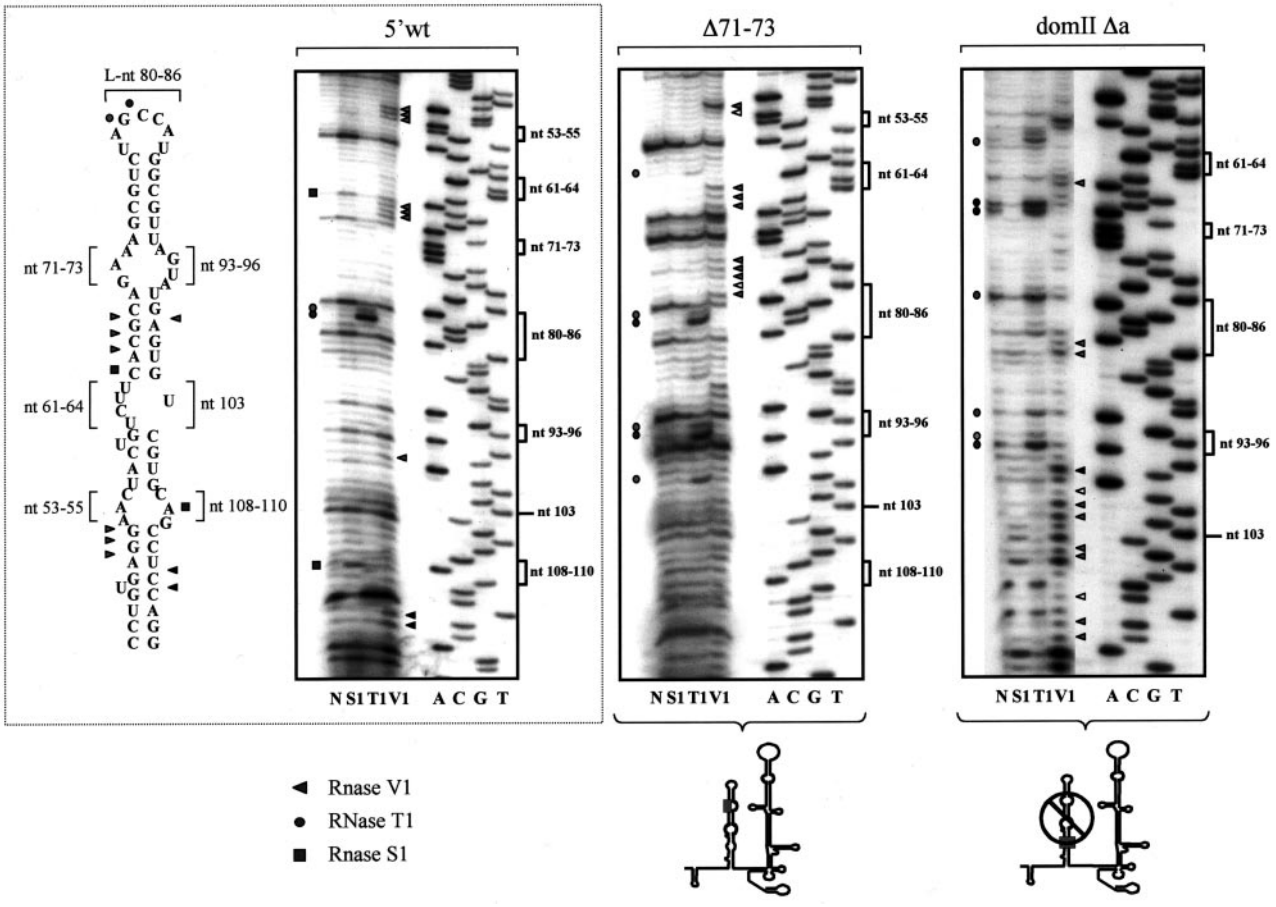

FIG. 7. **RNA secondary structure analysis of wild type and mutant domain II regions.** Enzymatic determination of the RNA secondary structure of HCV 5′-UTR domain II for the wild type sequence (5′-wt) and the two mutants Δ71-73 and domIIΔa was performed. *In vitro* transcribed RNA was enzymatically digested with S1 nuclease and T1 and V1 RNases and reverse-transcribed using a 5′-end-labeled oligonucleotide. The reverse transcription products were then separated on a 6% polyacrylamide sequencing gel. A sequencing reaction performed with the same primer was run in parallel to precisely determine the cleavage sites. *Squares, circles,* and *triangles* indicate S1 nuclease and T1 and V1 RNase cleavage sites, respectively. *Black* and *shaded symbols* indicate high and medium cleavage intensities. The *vertical bars* indicate the proposed bulge and loop regions of domain II. No enzyme was added to the reaction mixture in *lane N*. The observed cleavage sites in the wild type sequence (5′-wt) are reported on the proposed schematic diagram of domain II (*left panel*).

isolation of single-point mutations that do not appreciably affect HCV IRES activity has also been confirmed by the isolation of an HCV IRES quasispecies that contained four mutations in the bulge regions of domain II but whose translation efficiency was 80% that of the wild type (43). Moreover, deletions in the IIc bulge have shown a peculiar result: the double mutant domIIΔc retains a significant IRES activity, whereas deletion of only the right hand part of this bulge (Δ93-96) abolishes translation efficiency. This is a situation that is quite unlike what has been observed for other parts of the HCV IRES such as stem-loops IIId and IIIe (17, 27). A possible explanation for these observations may reside in the fact that the role played by domain II in HCV translation is, as suggested by Spahn *et al.* (13), predominantly structural. Indeed, we have performed UV cross-linking analyses on these mutants using different protein extracts (S100, nuclear extracts, ribosomal salt wash, and purified 40S subunit) to eventually identify cellular factors that bind domain II, but to date, we have not found any (data not shown), a result which, although not formal proof, adds to the existing evidence.

Interestingly, a recent genetic analysis (49) of a poliovirus/HCV chimera has proposed that the lower region of domain II may fold in an alternative conformation to the current model (8). The most notable difference between these two models resides in the nucleotide 108–110 region, which is in a stem position in the model by Zhao and Wimmer (49), whereas it is present in a single-stranded bulge conformation in the model by Honda *et al.* (8). Although both models are supported by phylogenetic and RNA prediction analysis, our nuclease S1 studies support the presence of A109 in a single-stranded status (see Fig. 7), in keeping with the structure proposed by Honda *et al.* (8). One possibility that may explain this discrepancy is that in the poliovirus/HCV chimera, the lower domain II region may fold differently as compared with our IRES constructs. However, it is also possible that both structures represent alternative foldings of domain II that may occur during the viral life cycle. In fact, changes in tertiary conformation may have important consequences for the recruitment of trans-acting factors to IRES domains, as recently reviewed in Ref. 4.

In conclusion, our findings support the recent model of HCV IRES-40S ribosomal subunit interaction (13) and the structural role played therein by domain II. In addition, our results identify the IIa bulge region as the most efficient target for antisense inhibition of HCV translation, a promising approach in the search for HCV-specific inhibitors (17, 50).

REFERENCES

1. Merrick, W. C., and Hershey, J. W. B. (1996) in *Translational Control* (Hershey, J. W. B., Mathews, M. B., and Sonenberg, N., eds), pp. 31–69, Cold Spring Harbor Laboratory, Cold Spring Harbor, NY
2. Jackson, R. J., Howell, M. T., and Kaminski, A. (1990) *Trends Biochem. Sci.* **15,** 477–483
3. Jackson, R. J. (2000) in *Translational Control of Gene Expression* (Hershey, J. W. B., Mathews, M. B., and Sonenberg, N., eds), pp. 127–184, Cold Spring Harbor Laboratory, Cold Spring Harbor, NY
4. Martinez-Salas, E., Ramos, R., Lafuente, E., and Lopez De Quinto, S. (2001) *J. Gen. Virol.* **82,** 973–984
5. Grace, K., Gartland, M., Karayiannis, P., McGarvey, M. J., and Clarke, B. (1999) *J. Gen. Virol.* **80,** 2337–2341
6. Rijnbrand, R., Abell, G., and Lemon, S. M. (2000) *J. Virol.* **74,** 773–783
7. Honda, M., Brown, E. A., and Lemon, S. M. (1996) *RNA* (*N. Y.*) **2,** 955–968
8. Honda, M., Beard, M. R., Ping, L. H., and Lemon, S. M. (1999) *J. Virol.* **73,** 1165–1174
9. Wang, C., Sarnow, P., and Siddiqui, A. (1994) *J. Virol.* **68,** 7301–7307
10. Wang, C., Le, S. Y., Ali, N., and Siddiqui, A. (1995) *RNA* (*N. Y.*) **1,** 526–537
11. Kieft, J. S., Zhou, K., Jubin, R., Murray, M. G., Lau, J. Y., and Doudna, J. A. (1999) *J. Mol. Biol.* **292,** 513–529
12. Lukavsky, P. J., Otto, G. A., Lancaster, A. M., Sarnow, P., and Puglisi, J. D. (2000) *Nat. Struct. Biol.* **7,** 1105–1110
13. Spahn, C. M., Kieft, J. S., Grassucci, R. A., Penczek, P. A., Zhou, K., Doudna, J. A., and Frank, J. (2001) *Science* **291,** 1959–1962
14. Kieft, J. S., Zhou, K., Jubin, R., and Doudna, J. A. (2001) *RNA* (*N. Y.*) **7,** 194–206
15. Kolupaeva, V. G., Pestova, T. V., and Hellen, C. U. (2000) *J. Virol.* **74,** 6242–6250
16. Klinck, R., Westhof, E., Walker, S., Afshar, M., Collier, A., and Aboul-Ela, F. (2000) *RNA* (*N. Y.*) **6,** 1423–1431
17. Jubin, R., Vantuno, N. E., Kieft, J. S., Murray, M. G., Doudna, J. A., Lau, J. Y., and Baroudy, B. M. (2000) *J. Virol.* **74,** 10430–10437
18. Rijnbrand, R., Bredenbeek, P., van der Straaten, T., Whetter, L., Inchauspe, G., Lemon, S., and Spaan, W. (1995) *FEBS Lett.* **365,** 115–119
19. Buratti, E., Gerotto, M., Pontisso, P., Alberti, A., Tisminetzky, S. G., and Baralle, F. E. (1997) *FEBS Lett.* **411,** 275–280
20. Buratti, E., Tisminetzky, S., Zotti, M., and Baralle, F. E. (1998) *Nucleic Acids Res.* **26,** 3179–3187
21. Odreman-Macchioli, F. E., Tisminetzky, S. G., Zotti, M., Baralle, F. E., and Buratti, E. (2000) *Nucleic Acids Res.* **28,** 875–885
22. Fukushi, S., Kurihara, C., Ishiyama, N., Hoshino, F. B., Oya, A., and Katayama, K. (1997) *J. Virol.* **71,** 1662–1666
23. Tang, S., Collier, A. J., and Elliott, R. M. (1999) *J. Virol.* **73,** 2359–2364
24. Hwang, L. H., Hsieh, C. L., Yen, A., Chung, Y. L., and Chen, D. S. (1998) *Biochem. Biophys. Res. Commun.* **252,** 455–460
25. Varaklioti, A., Georgopoulou, U., Kakkanas, A., Psaridi, L., Serwe, M., Caselmann, W. H., and Mavromara, P. (1998) *Biochem. Biophys. Res. Commun.* **253,** 678–685
26. Hellen, C. U., and Pestova, T. V. (1999) *J. Viral Hepat.* **6,** 79–87
27. Psaridi, L., Georgopoulou, U., Varaklioti, A., and Mavromara, P. (1999) *FEBS Lett.* **453,** 49–53
28. Rijnbrand, R. C., Abbink, T. E., Haasnoot, P. C., Spaan, W. J., and Bredenbeek, P. J. (1996) *Virology* **226,** 47–56
29. Reynolds, J. E., Kaminski, A., Kettinen, H. J., Grace, K., Clarke, B. E., Carroll, A. R., Rowlands, D. J., and Jackson, R. J. (1995) *EMBO J.* **14,** 6010–6020
30. Reynolds, J. E., Kaminski, A., Carroll, A. R., Clarke, B. E., Rowlands, D. J., and Jackson, R. J. (1996) *RNA* (*N. Y.*) **2,** 867–878
31. Pestova, T. V., Shatsky, I. N., Fletcher, S. P., Jackson, R. J., and Hellen, C. U. (1998) *Genes Dev.* **12,** 67–83
32. Sizova, D. V., Kolupaeva, V. G., Pestova, T. V., Shatsky, I. N., and Hellen, C. U. (1998) *J. Virol.* **72,** 4775–4782
33. Ali, N., Pruijn, G. J., Kenan, D. J., Keene, J. D., and Siddiqui, A. (2000) *J. Biol. Chem.* **275,** 27531–27540
34. Ali, N., and Siddiqui, A. (1997) *Proc. Natl. Acad. Sci. U. S. A.* **94,** 2249–2254
35. Isoyama, T., Kamoshita, N., Yasui, K., Iwai, A., Shiroki, K., Toyoda, H., Yamada, A., Takasaki, Y., and Nomoto, A. (1999) *J. Gen. Virol.* **80,** 2319–2327
36. Hahm, B., Kim, Y. K., Kim, J. H., Kim, T. Y., and Jang, S. K. (1998) *J. Virol.* **72,** 8782–8788
37. Fukushi, S., Okada, M., Kageyama, T., Hoshino, F. B., Nagai, K., and Katayama, K. (2001) *Virus Res.* **73,** 67–79
38. Spangberg, K., and Schwartz, S. (1999) *J. Gen. Virol.* **80,** 1371–1376
39. Ali, N., and Siddiqui, A. (1995) *J. Virol.* **69,** 6367–6375
40. Anwar, A., Ali, N., Tanveer, R., and Siddiqui, A. (2000) *J. Biol. Chem.* **275,** 34231–34235
41. Kaminski, A., Hunt, S. L., Patton, J. G., and Jackson, R. J. (1995) *RNA* (*N. Y.*) **1,** 924–938
42. Honda, M., Kaneko, S., Matsushita, E., Kobayashi, K., Abell, G. A., and Lemon, S. M. (2000) *Gastroenterology* **118,** 152–162
43. Laporte, J., Malet, I., Andrieu, T., Thibault, V., Toulme, J. J., Wychowski, C., Pawlotsky, J. M., Huraux, J. M., Agut, H., and Cahour, A. (2000) *J. Virol.* **74,** 10827–10833
44. Brown, E. A., Zhang, H., Ping, L. H., and Lemon, S. M. (1992) *Nucleic Acids Res.* **20,** 5041–5045
45. Fukushi, S., Okada, M., Kageyama, T., Hoshino, F. B., and Katayama, K. (1999) *Virus Genes* **19,** 153–161
46. Fukushi, S., Okada, M., Stahl, J., Kageyama, T., Hoshino, F. B., and Katayama, K. (2001) *J. Biol. Chem.* **276,** 20824–20826
47. Buratti, E., Baralle, F. E., and Tisminetzky, S. G. (1998) *Cell. Mol. Biol.* (*Noisy-le-grand*) **44,** 505–512
48. Buratti, E., Di Michele, M., Song, P., Monti-Bragadin, C., Scodeller, E. A., Baralle, F. E., and Tisminetzky, S. G. (1997) *Clin. Diagn. Lab. Immunol.* **4,** 117–121
49. Zhao, W. D., and Wimmer, E. (2001) *J. Virol.* **75,** 3719–3730
50. Di Bisceglie, A. M. (1999) *Am. J. Med.* **107,** 45S–48S

Mutational Analysis of the Different Bulge Regions of Hepatitis C Virus Domain II and Their Influence on Internal Ribosome Entry Site Translational Ability

Federico Odreman-Macchioli, Francisco E. Baralle and Emanuele Buratti

J. Biol. Chem. 2001, 276:41648-41655.
doi: 10.1074/jbc.M104128200 originally published online August 9, 2001
